HOSTED BY
ELSEVIER
Available online at www.sciencedirect.com
ScienceDirect
Soils and Foundations 61 (2021) 239–255
www.elsevier.com/locate/sandf

Geo-Disaster Report

Large distance flow-slide at Jono-Oge due to the 2018 Sulawesi Earthquake, Indonesia

Hemanta Hazarika [a,*], Divyesh Rohit [a], Siavash Manafi Khajeh Pasha [b], Tsubasa Maeda [a], Irsyam Masyhur [c], Ardy Arsyad [d], Sukiman Nurdin [e]

[a] Department of Civil Engineering, Kyushu University, Fukuoka, Japan
[b] IMAGEi Consultant, Tokyo, Japan
[c] Faculty of Civil and Environmental Engineering, Bandung Institute of Technology, Bandung, Indonesia
[d] Department of Civil Engineering, Hasanuddin University, South Sulawesi, Indonesia
[e] Department of Civil Engineering, Tadulako University, Central Sulawesi, Indonesia

Received 27 January 2020; received in revised form 23 September 2020; accepted 8 October 2020
Available online 24 November 2020

Abstract

There was a shallow earthquake in the Central Sulawesi province of Sulawesi island of Indonesia with a moment magnitude (Mw) 7.5 on 28th September 2018 at 18:02:44 local time. The event was preceded by major foreshocks and followed by aftershocks of significant magnitude. The epicenter of the main shock was in the Donggala regency of Minahasa peninsula of Central Sulawesi, approximately 70 km from the provincial capital of Palu. The earthquake was caused by the tectonic movement of the left lateral Palu- Koro fault within the Molucca Sea microplate, triggering major geotechnical failure and structural damage in Palu city and Sigi regency. Thousands of people died or are still unaccounted for, and countless others were injured. Balaroa, Petobo, Jono-Oge and Sibalaya were the worst hit mainly due to large-scale flow-slides and mud flows. It was the first time that such large-scale flow failures were triggered by an earthquake, and that the failure of very gentle sloping ground swept away whole localities. The objective of this research was to provide insight into the scale of ground failure and other infrastructural damage caused by the event, especially in Jono-Oge area, where the flow distance was longest. The authors performed preliminary and detailed surveys in the area twice by conducting Portable Dynamics Cone Penetration Test (PDCPT), collecting disturbed and undisturbed samples and using aerial drone (UAV) photography. The findings of the reconnaissance survey are described here along with subsequent data interpretation. Finally, the mechanism of the flow-slides is discussed.

Keywords: Flow-slide; Large distance flow; Liquefaction; Water film; Dynamic cone penetration test; Drone survey

1. Introduction

Being situated at the conjuncture of highly active Australian, Pacific, Sunda and Philippine Sea plates, the Sulawesi Island in Eastern Indonesia is not new to seismic events of significant magnitude. On September 28, 2018, the region was struck by a large earthquake of moment magnitude Mw 7.5 at 18:02:44 local time, which triggered devastating large-scale flow failures and a tsunami. The epicenter of earthquake was located at 0.256°S (latitude) and 119.846°E (longitude) in the Donggala regency of Minahasa peninsula, about 70 km north of the provincial capital of Palu with a hypo-central depth of 20 km (USGS, 2018). The earthquake had a peak intensity of 8.5 on the MMI scale, as observed in Palu region. The event was preceded by a major foreshock of magnitude

Peer review under responsibility of The Japanese Geotechnical Society.
* Corresponding author.
E-mail address: hazarika@civil.kyushu-u.ac.jp (H. Hazarika).

https://doi.org/10.1016/j.sandf.2020.10.007
0038-0806/

Mw 6.1 just hours before the main shock and followed by multiple aftershocks of magnitude $M_w > 5.5$ for more than a week. The tremors of the main shock were felt as far away the Eastern Kalimantan region of Borneo Islands as well as in Tawau district in Malaysia. The extensive damage to the transportation systems, bridges, earth structures and residential buildings in some areas of Palu city, Sigi and Donggala regency of Central Sulawesi was due to the widespread large-scale flow failures (Mason et al., 2019). Along with destruction to infrastructure, thousands of lives were lost, many more were injured and hundreds were reported missing (Mikami et al., 2019; Omira et al., 2019). Balaroa, Petobo, Jono-Oge and Sibalaya were the worst hit mainly due to large-scale flow-slides and mud flows. Never before have such large-scale flow failures been triggered by an earthquake. That these failures occurred on very gentle sloping ground, sweeping away localities along with it, came as a complete surprise to one and all.

The long-distance flow failures are thought to have resulted from a combination of many factors, including the liquefaction of the sandy layer, the formation of water film due to the existence of a less-permeable cap layer, the presence of a confined aquifer, and the geology typical of the affected areas (Kiyota et al., 2020). The reconnaissance survey was designed to determine the role of these factors in the disaster. Perishable data was collected to supplement knowledge of earthquake induced geo-disasters, in the expectation that this would ultimately lead to improved procedures for the characterization and mitigation of geo-hazard risks. In this paper, the focus is on the results of the reconnaissance survey of the events of this extreme geo-disaster in the wake of the 2018 Sulawesi earthquake during November 2 to 4, 2018 and June 26 to July 4, 2019. The approach adopted was similar to the traditional reconnaissance methods used to collect earthquake records, field testing on geotechnical and geological ground conditions, and advanced aerial imaging using unmanned aerial vehicles (UAV).

The field reconnaissance of earthquake-induced liquefaction and associated ground failures contributes significantly towards the knowledge and advancing understanding of the behavior and the mechanics of liquefied ground. The careful documentation and assessment of observations from many liquefied and non-liquified sites during past extreme events have provided us with a valuable database of case histories (Andrus and Stokoe, 2000; Cetin et al., 2004; Moss et al., 2006, 2011; Boulanger et al., 2012; Ohsumi et al., 2016), lateral spreading (Bardet et al., 2002; Youd et al., 2002; Cubrinovski et al., 2012) and post liquefaction ground subsidence (Cetin et al., 2009; Juang et al., 2013; Valverde-Palacios et al., 2014). However, acquiring reliable, good quality, documented liquefaction reconnaissance data from sites right after an earthquake can be extremely challenging, since strong ground motion tends to occur over a very large geographical area. On the other hand, recent advances in computer simulations and unmanned aerial vehicles (UAV) provide an excellent opportunity to access the remote areas that have suffered earthquake induced damage to collect perishable surface geotechnical data for analysis.

Our research team visited sites in Jono Oge village in Palu to assess the damage caused by the large scale flow failure triggered by the earthquake and to observe the sub-soil conditions. The village of Jono Oge was selected in this survey because it had the largest magnitude of ground displacement due to the flow-slides among the all other sites in Palu city.

The reconnaissance survey methods included visual site inspection, collecting disturbed and undisturbed soil samples, performing portable dynamic cone penetration tests (PDCPT) for in-situ soil strength assessment and conducting aerial survey using drone to obtain an overall high-resolution top view of the site with terrain information. The team also investigated the soil profiles in the trenches excavated (Okamura et al, 2020; JICA, 2019) in the failed zones at Jono Oge village as well as in some other areas, such as Lolu and Sibalaya. The objective of the survey was to collect perishable field data and evaluate the probable causes and mechanism, which triggered such large-scale ground movement in such gently sloped ground.

2. Geological and seismological information of site

2.1. Event characteristics

With multiple active strike slip faults and subduction zones in the region, Sulawesi tends to be a complex seismically active zone. The province was struck by a powerful earthquake of magnitude M_w 7.5 on 28 September 2018 with strong foreshocks and aftershocks. The map of Central Sulawesi area shown in Fig. 1 indicates the locations of the foreshocks, the main shock and aftershocks of the 2018, Sulawesi earthquake. The data for the event history is considered from September 28, 2018 to October 08, 2018. It can be seen from the magnitude of the foreshocks and the aftershocks indicated in Fig. 1 that a lot of energy was accumulated across the Palu-Koro fault. There was a foreshock of magnitude Mw 6.1 approximately 3 h before the main event of magnitude Mw 7.5 and the aftershocks which followed the event for days were of significant magnitude, most of them greater than Mw 5.

The event caused large scale liquefaction and lateral flow failures across the villages of Jono-Oge, Sibalaya, Petobo and Balaroa, with the largest flow failure observed in Jono-Oge (Bradley et al., 2019; Watkinson and Hall, 2019; Cummins, 2019). Fig. 2a. shows the epicenter along with the locations of large-scale flow failures along with the sinistral Palu-Koro Fault (PKF), which caused the earthquake. Fig. 2b. depicts the intensity contours of Palu city along with the liquefaction susceptibility map for the September 28, Sulawesi Earthquake. The map indicates that the event had maximum intensity in Palu valley with the highest liquefaction susceptibility despite being almost 70 km from the epicenter. Fig. 2c & d are the satellite

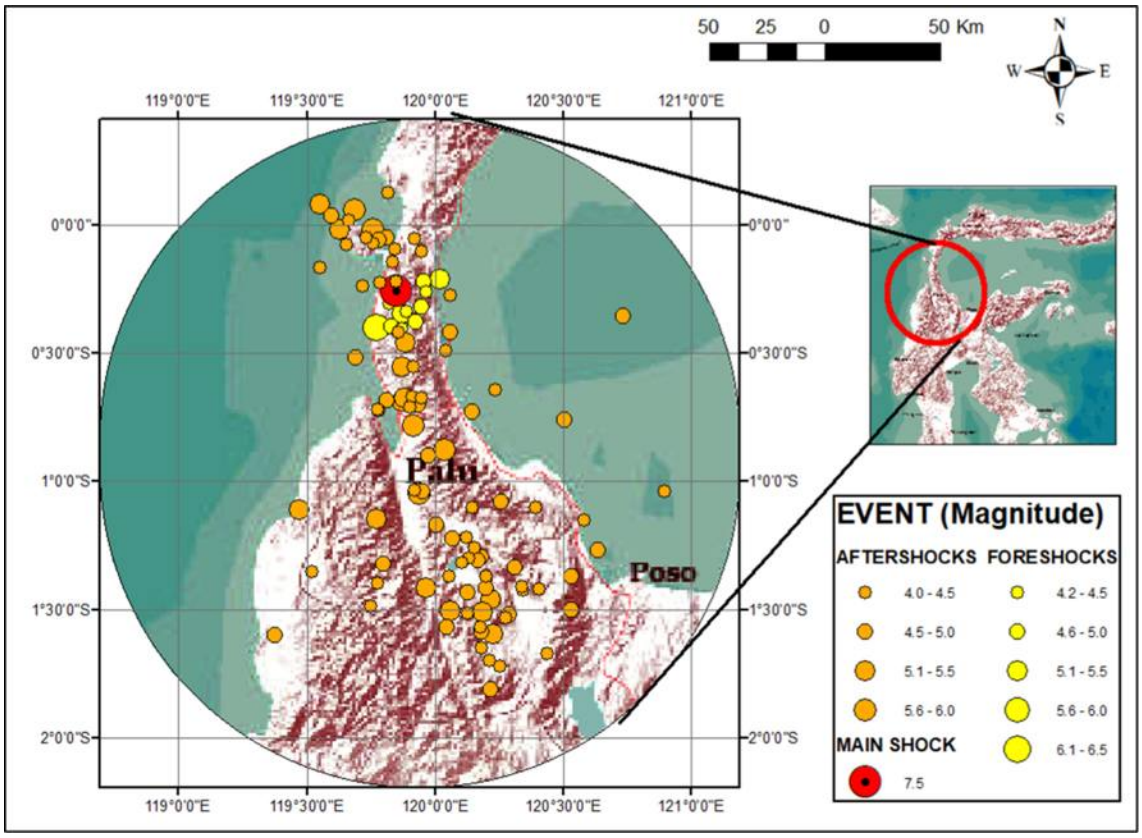

Fig. 1. Location of foreshocks, mainshock, and aftershocks with varying magnitude.

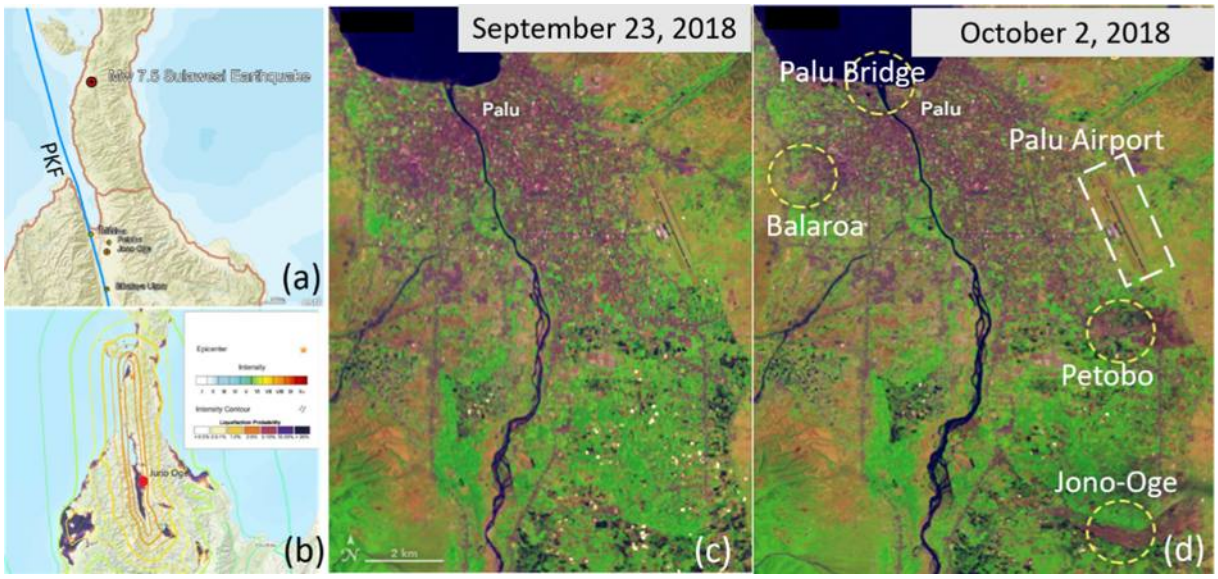

Fig. 2. Intensity Map and ground failures associated with Mw 7.5 Palu earthquake (a) Epicenter of The 2018 Sulawesi earthquake along locations of flow failure and alignment of Palu-Koro fault (b) Intensity contour with liquefaction probability map of Palu city (USGS, 2018), (c) Landsat 8 image taken on September 23, 2018 and (d) Landsat 8 image taken on October 2, 2018 (showing the sites with major flow failure damages; USGS, 2018).

images acquired on September 23, 2018 and October 2, 2018 respectively by Operational Land Imager (OLI) on Landsat 8 satellite (USGS, 2018) in false color bands (6-5-2) to make it easy to differentiate between the urban areas (purple-gray), vegetation (green), and over-turned soil (brown and tan). On observing both Fig. 2c & d, the mud flow and debris can be easily identified which occurred due to liquefaction induced flow failure. Furthermore, the images in Fig. 2c & d indicate that there was no notable damage to Palu airport, which is located near the flow

failure site of Petobo. This may be due to ground improvement measures implemented during the construction of the airport.

2.2. Site characteristics

The Central Sulawesi province is straddled by the seismically active left lateral Palu -Koro fault (PKF). On September 28, due to the 2018 Sulawesi earthquake, several meters of horizontal crustal displacement were observed across the PKF, confirmed through satellite image analysis (Heidarzadeh et al., 2019). All the large-scale flow-slides sites were found to lie across or near the fault zone.

In this research, the site reconnaissance activities were focused on the area of interest (Jono Oge village), where the maximum displacement of soil mass of distances up to 1 km was observed. Jono Oge is located in Palu region in Central Sulawesi province of Sulawesi island, which is one of the largest islands of Indonesia. Because it covers such a vast area across both sides of equator and inside the area of the ring of fire, the tectonic activities of Indonesia are complex, with all the tectonic activities represented, including subduction, collision, uplift, strike-slip faulting and volcanic activities (Hall, 2014).

Being the most active fault in the Sulawesi region, PKF has an average slip rate of 40 mm/year, and has an extension rate of ~11–14 mm/year, which is quite complex for a simple strike-slip fault (Socquet et al., 2006). The region is overlain by sedimentary and volcanic deposits of Miocene – Quaternary period, which have undergone low grade thermal metamorphism (van Leeuwen et al., 2016). The Palu valley extends 7 km in width and is flanked by N-S aligned, sharp triangular slopes about 60 m in height and short alluvial fans to the West, and gentle steps faults to the East (Thein et al., 2015). Hosting an active strike – slip fault, the region has experienced multiple large devastating earthquakes in the past. The historic seismicity of the PKF region shows that the fault activity is concentrated at shallow depths with major earthquakes of magnitude $Mw \geqslant 6.5$ during years 1900–2018 with a hypocentral depth of less than 50 km, (Socquet et al., 2006), as shown in Fig. 3(a) and (b).

2.3. Geology and tectonic characteristics

The basement rock in the region where the Palu city is located (near the neck) and connects western part of central Sulawesi to north arm are formed by several metamorphic complex covered by magmatic intrusion with different composition varied from gabbro and diorite to granite and volcanic sedimentation (Watkinson et al., 2011). The bedrock geology map of Palu is shown in Fig. 4. The Palu Basin is overlain with Quaternary sediments (Fig. 5), which are very young in age. Flood deposits from irrigation channel in the slide areas and alluvial flood constitute clay, silt, and sand. Surficial sediments are formed by young alluvium fan deposits in low relief hills which extend up the west and east sides of the valley. Foothills and mountains which surrounded the Palu valley constitute tertiary granite and granodiorite rock and pre-tertiary sedimentary and metamorphic rock. A past study on the sedimentary deposits of Ariana region confirmed that the young sedimentary deposits are susceptible to liquefaction, with a shallow ground water table and under 0.2 g ground motion acceleration (El May et al., 2009). While the event in Palu reflects all the above criteria, a more detailed site-specific study was required to confirm the details of the slope failure triggered by the 2018 earthquakes.

2.4. Ground motion characteristics

The very high rupture velocity of the 2018 Palu earthquake contributed to the large intensity of ground motion, and led to it being categorized as a super-shear event (Socquet et al., 2019). Ground motion data of earthquake was recorded at the JICA-BMGK station in Palu, which is approximately 80 km from the epicenter and on the west side of earthquake induced landslide area at Balaroa (Fig. 6). The time history of acceleration for two horizonal components E-W and N-S and vertical component U-D of ground motion is shown in Fig. 7, using the data provided in Kiyota et al. (2020). The peak ground acceleration (PGA) values of the E-W, N-S and U-Components were 0.28 g, 0.21 g, and 0.34 g respectively.

The response spectra shown in Fig. 7d display near-fault motion features likely to have been caused by forward directivity of rupture propagation. Furthermore, the wide range frequency content of ground motion increased the risk of geotechnical failure at various places. However, the response spectral values at the Palu station were reported to be less than those proposed by the Indonesian seismic design code, except for the period range of 2.5–3.5 s (Goda et al., 2019).

3. Earthquake induced flow-slides in Palu region

3.1. Geotechnical site investigations

The 2018 Sulawesi earthquake triggered four large scale flow-slides (Balaroa, Petobo, Jono Oge and Sibalaya) which are located in the vicinity of Palu city (Fig. 8). The slide areas are all located along the edges of Palu valley, where the new alluvial fans meet the old alluvial fan deposits of Palu river. The landslide in Balaroa (northwest side of Palu valley) was on gentle ground with average slope of 4% and partially or fully damaged approximately 2,900 residential buildings. The other three flow-slides in Petobo, Jono Oge and Sibalaya were in the east side of Palu valley within the 25 km of Palu city. According to reports and the damage mapping provided by Copernicus Emergency Management Service, flow-slides damaged or destroyed more than 300 buildings in Jono-Oge and 3,000 buildings in Petobo. More than 140 buildings in Sibalaya were damaged.

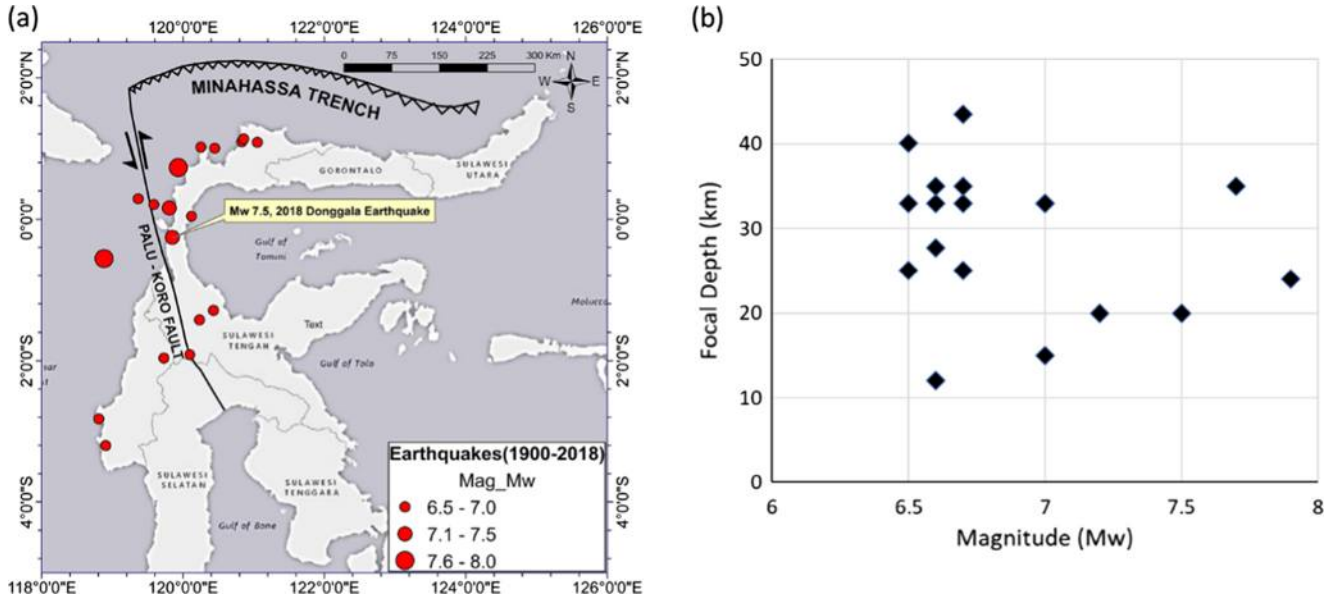

Fig. 3. Distribution and magnitude of PKF (1900–2018) (a) Earthquakes across the Sulawesi island (Mw⩾6.5) (b) Hypocentral depth (km) for the same events (USGS, 2018, Socquet et al., 2006).

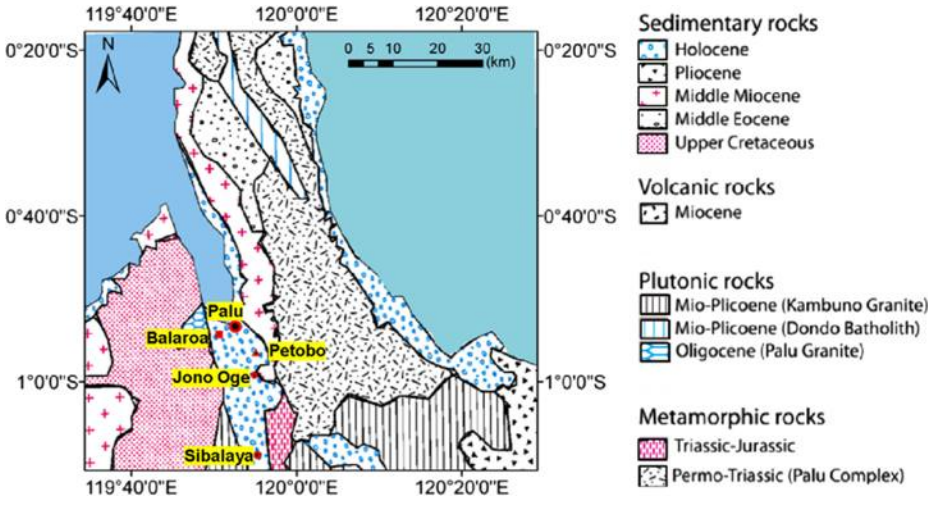

Fig. 4. Geologic map of the Palu area (modified from Watkinson et al., 2011).

In this study, we used a combination of satellite imagery, aerial imagery, field surveys including collecting soil samples from the sites and conducting in-situ testing using Portable Cone Penetrometer, to investigate the mechanism of massive flow-slides. The discussion in the following subsections is mainly focused on the mechanism and patterns of mass movements in the Jono-Oge area, which was the largest flow failure (in terms of area and volume) in the region after the event.

3.2. Flow-slide at Jono-Oge

As shown in Fig. 9a and b, the flow-slide in Jono Oge started from the crown next to irrigation channel in eastern edge of Palu valley to the toe deposits on the western side of failure zone. The slide spread over 1.5 km^2 of area with maximum displacement of 2 km. The slide swept away the residential buildings as well as the connecting roads between the north and south of Jono Oge with huge deposition of residuals on top of the sliding surface. It should be noted that the over 90% of the area where the flow-slide occurred was agriculture farms. A high ground water level and underground water in the surficial sandy layers due the presence of irrigation channel likely exacerbated the ground conditions, and contributed significantly to the large scale flow-slide, which extended over a number of kilometers.

3.2.1. Satellite and drone imagery

We used Unmanned aerial vehicle (UAV) to collect the digital images of the flow-slide Since no UAV imagery data of the pre-earthquake morphological features was avail-

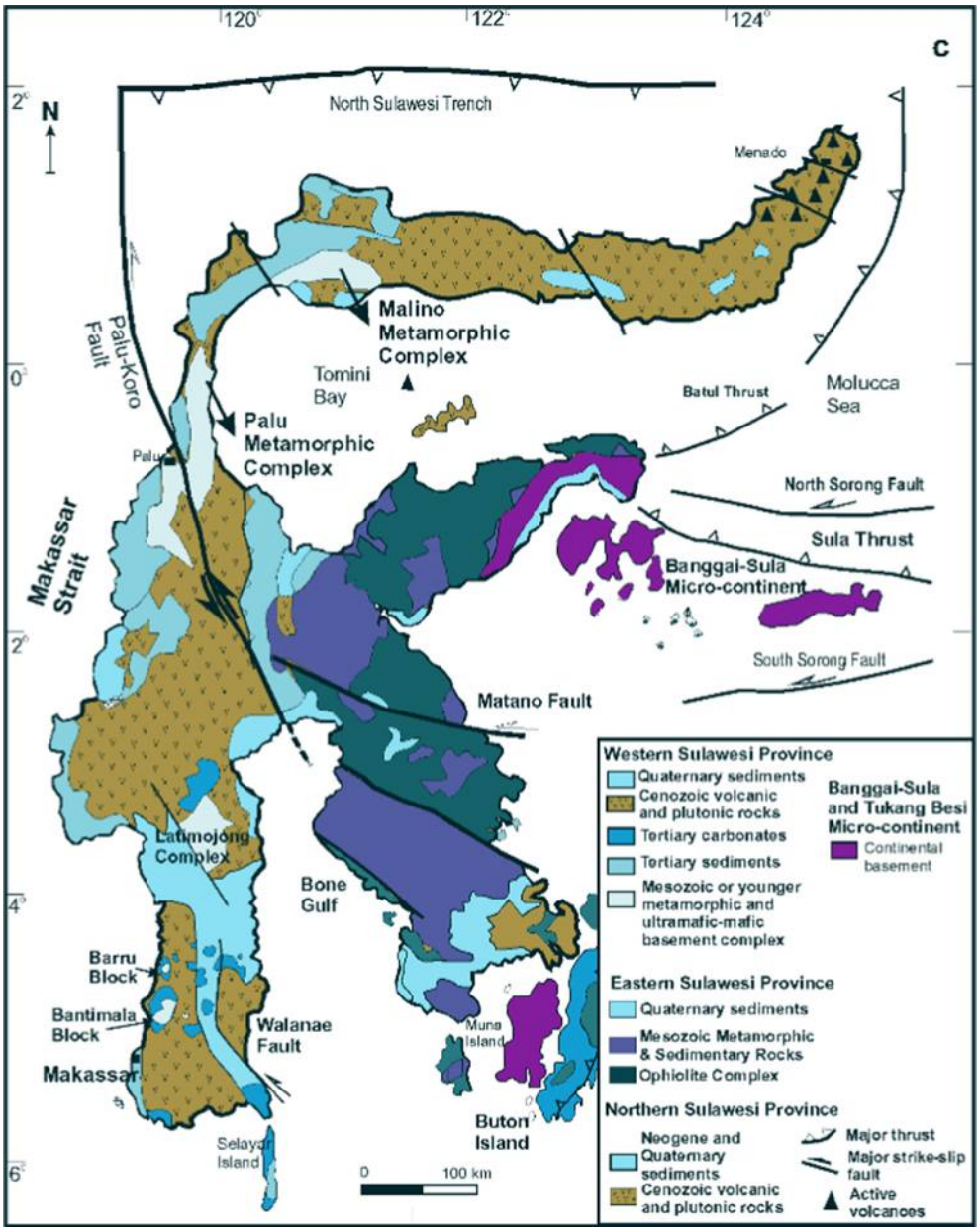

Fig. 5. Structures and geographical features of central Sulawesi region, Indonesia (Maulana et al., 2016).

able, the locations of structures and satellite imagery was used to identify those features. The post-earthquake displacements and changes in the morphological features of the area were clearly identified by this combination of information. The area was categorized into our different zones I, II, III and IV, as shown in Fig. 10.

Zone (I): The lands enclosed by Zone (I) are mainly rice and tomato fields with a few numbers of residential buildings. Being the crown (head scrap) of the flow-slide region, Zone (I) extends from northeast side of the failure zone along the western boundary of the irrigation channel to the southeast side, where the failure zone intersects with the channel. The breach of the channel and the destruction of the water gate resulted in the discharge of a huge volume of water, resulting in the scouring of the neighboring failure bed, as shown in Fig. 11. The subsequent mudflow carried the soil residuals all the way down to the Palu river [Fig. 11]. The flow-slide in zone (II) resulted in the development of extensional cracks, and the rotation and transmission of individual blocks of surficial soils (Fig. 12a). The maximum displacement of soils in this zone varies between 2 and 50 m.

1- Zone (II): The flow-slide began in this zone, and then scouring, erosion and lateral displacement followed. After the onset of liquefaction in the sandy and sandy-silty layers below the ground surface, the top surficial layers started moving in the southwest direction of the failure zone. It carried the soil blocks and residuals along with the runout and deposited them in

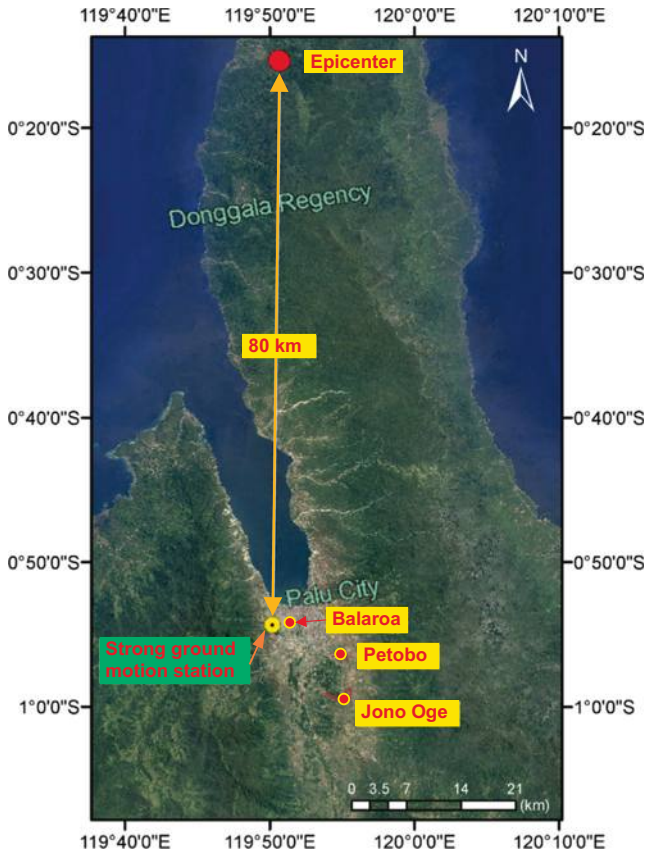

Fig. 6. JICA-BMGK strong motion station (JICA Report, 2019).

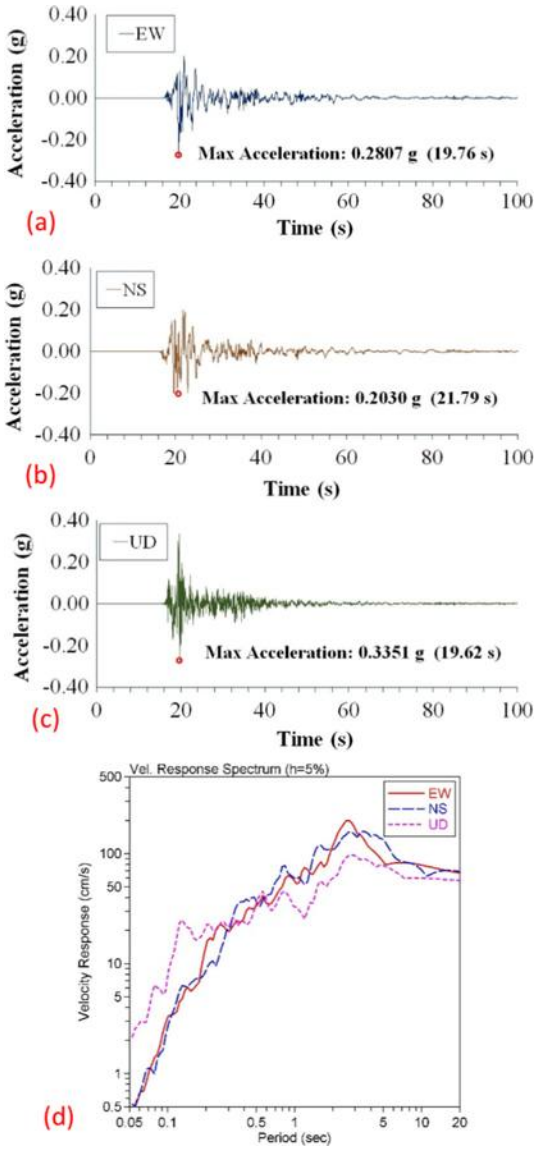

Fig. 7. Time history of motions at strong ground motion station near Balaroa (a) E-W (b) N-S (c) U-D components and (d) Velocity responses (Adopted and modified from the data in JICA Report, 2019).

Zone (III) (see below). Since the mudflow that resulted from the breached channel disturbed the tracing of the transition, the exact direction of soil movement remains largely unknown. Also, the erosion caused by the flood from the breached channel disturbed the surface morphology in this region, as seen in Fig. 12b. The severely eroded areas are devoid of any vegetation, while the surrounding areas are still vegetated. In order to map the displacement in this region, the movement of several structures on the less disturbed blocks was evaluated. The maximum displacement in this region varied from 300 to 1,300 m. An example of large-scale movement of structures on a soil block is shown in Fig. 12c, where a residential building (with blue roof) was transported by about 480 m from its original location on the eastside of failure zone.

2- Zone (III): The deposits of the flow-slide area were collected in this zone as well as the residuals of the rubble and trees which were transported from Zone (II). The transportation distance of soil deposits from zone (III) to zone (IV) due to the mudflow (yellow colored highlighted area in Fig. 10) is not clear. Some of the structures were carried by 1,200 m from the west of the flow-slide region. The mudflow resulted in the pile-up of runouts deposits a few meters in depth in this region (Fig. 12d).

3- Zone (IV): As explained above, the flow-slide in Zone (II) breached the walls of the irrigation channel, resulting in the flow of flood water through Zone (I) and Zone (II) until it joined the stream in the north and traveled the same path to Palu river.

3.2.2. *In-situ tests*

In-situ tests using the Portable Dynamic Cone Penetrometer Tests (called hereafter PDCPT) were performed to clarify the mechanism and progression of long-distance flow-slide at Jono Oge. Soil samples were also collected from the flow-slide sites for testing. The PDCPT equipment specifications and test procedures used in this research are in accordance with the Japanese Geotechnical Society Standard (2016). These field tests, together with laboratory

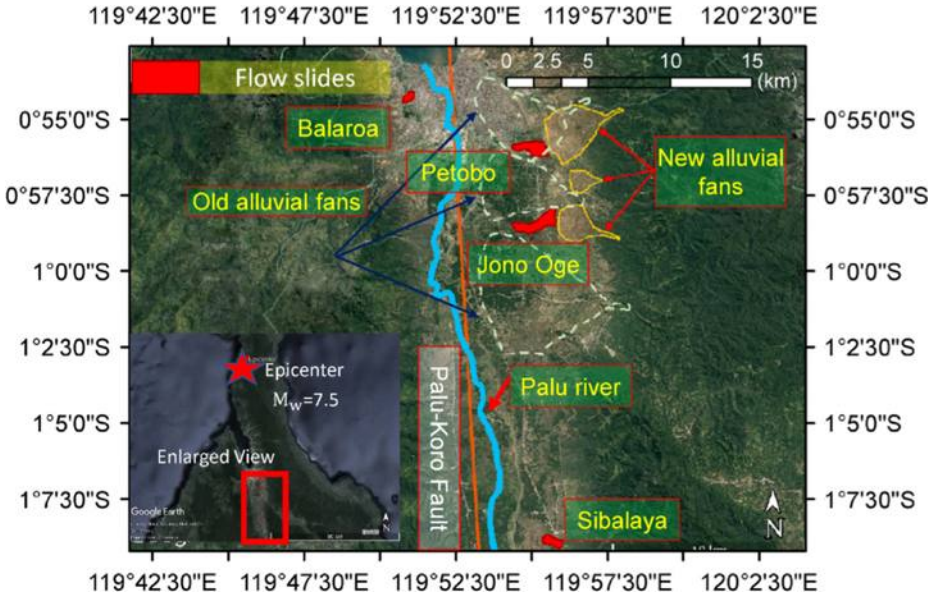

Fig. 8. Locations and extent of flowslides in different areas of Palu valley.

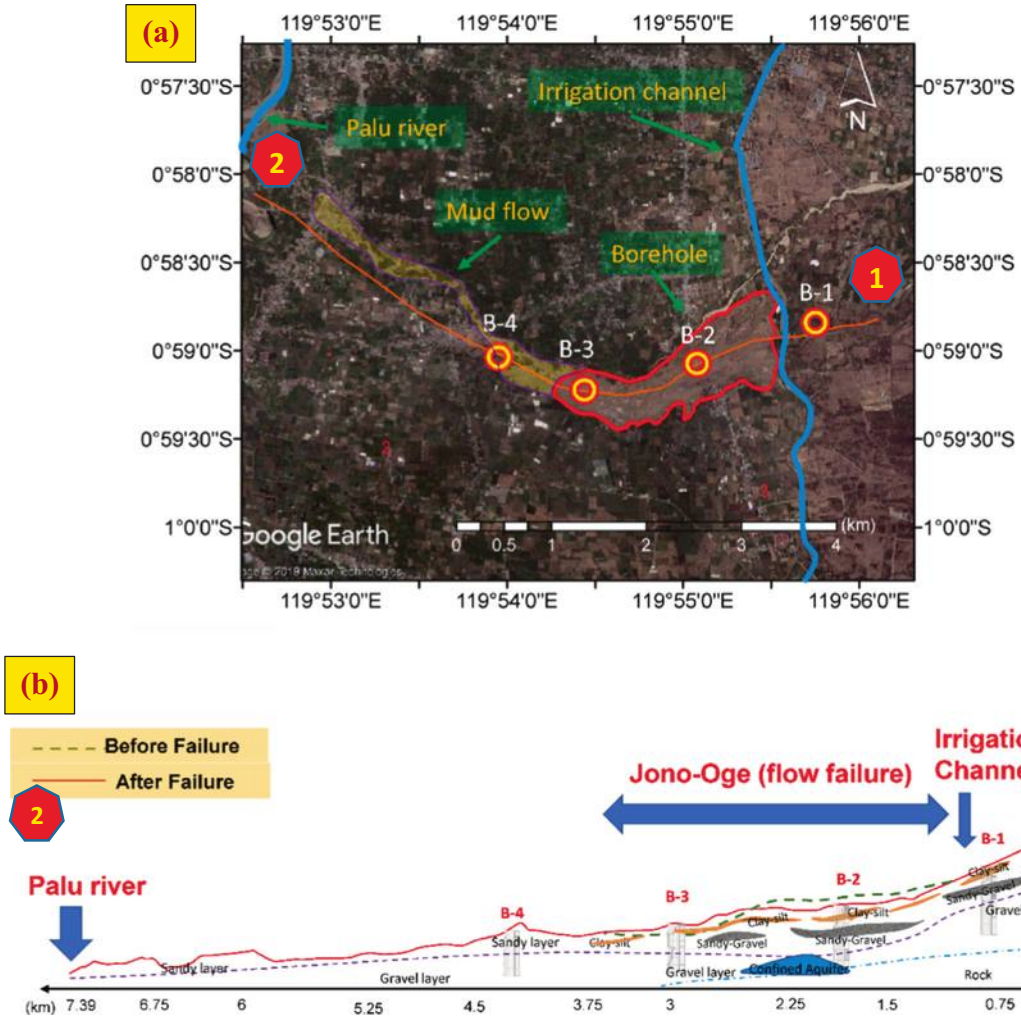

Fig. 9. Satellite imagery and ground profile (a) Flow slide after earthquake (c) Cross section at profile 1–2 (Not to scale).

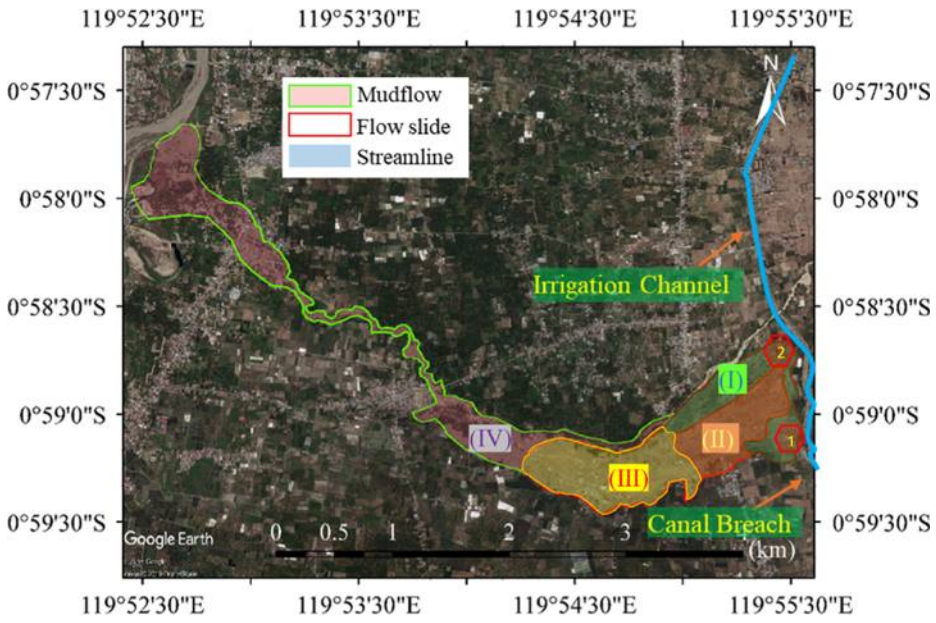

Fig. 10. Divided zones based on ground displacement in flowslide area.

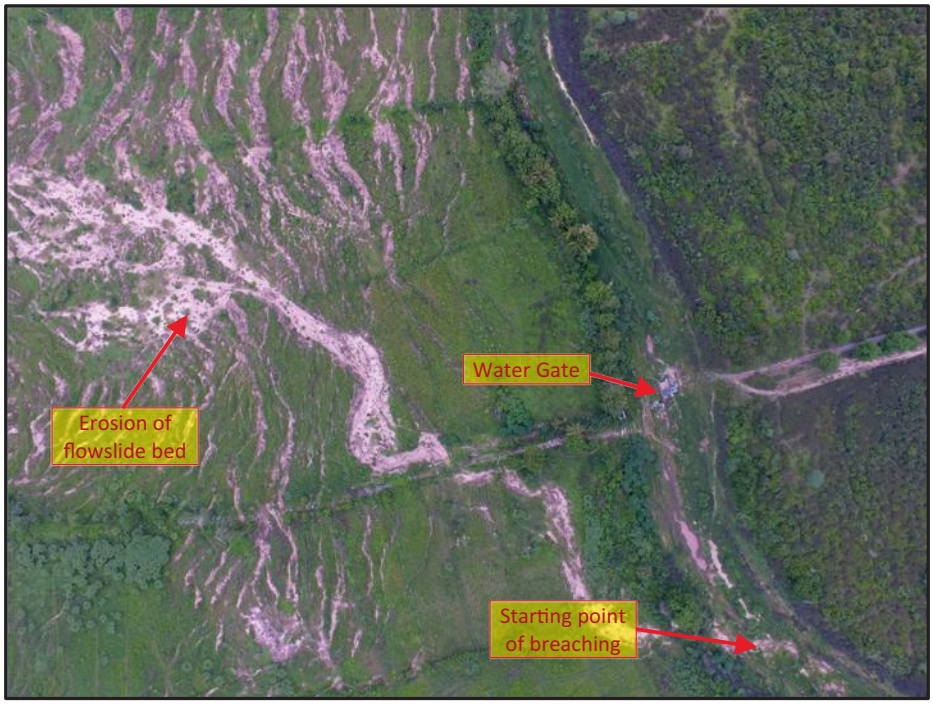

Fig. 11. UAV imagery of channel breaching and water gate destruction in Jono Oge (Location No. 1 of Fig. 10).

testing of the collected soil samples and visual observation of site condition, were expected to provide valuable information on the subsurface properties.

Fig. 13 shows the locations of the sites where soil samples were collected and PDCPT were conducted. As can be seen from the figure, the locations for the PDCPTs (PDCPT1, PDCPT4, PDCPT5, PDCPT6, PDCPT8) were selected such to ensure various locations with different characteristics were included: within the flow-slide zones (zones (I) and (II)) and outside of the flow-slide zone in North-South (alongside the damaged main access road connecting North to south of Jono-Oge) and in the South-North-East directions.

3.2.2.1. Results from the tests conducted outside the flow-slide zone. A PDCPT1 was conducted outside the failure zone on the margin far from the extensional cracks. Since the original stratification of ground is well preserved

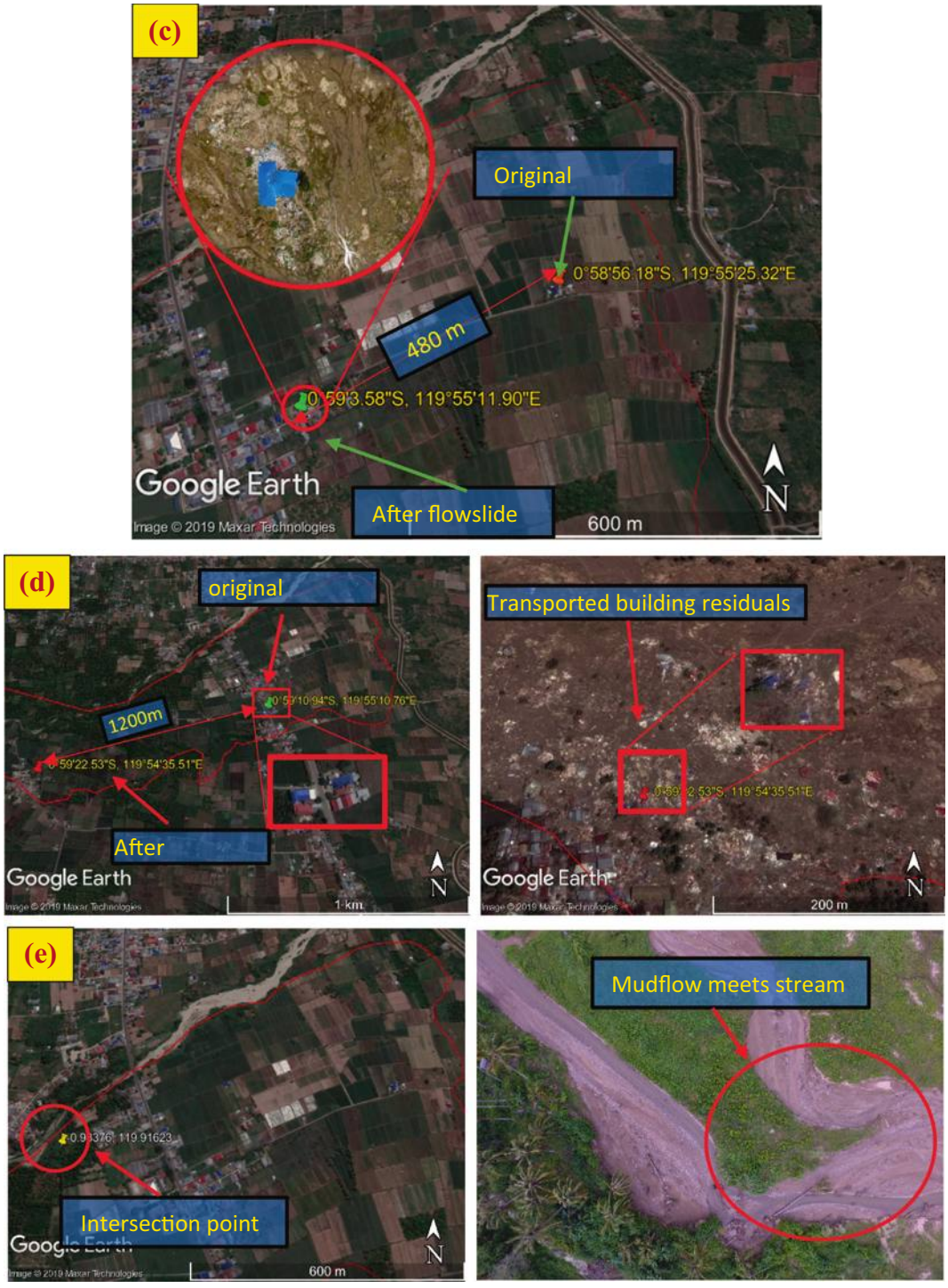

Fig 12. *(continued)*

outside of flow-slide area, the result of PDCPT1 was used as a benchmark for evaluating the results of the PDCPT tests within failure zones (II) and (I).

Fig. 14a shows the aerial view of the PDCPT1 location and the resulting N-values, which varied with depth. The test was conducted on an agriculture farm (with paddy fields and a tomato farm). The clear decrease in the N value in the soil layers below 3.5 m is an indication of loose liquefiable layers. The very high ground water level (which was higher than the water level at the time of testing G. W. L = 2.3 m) also contributes to and increased risk of liquefaction in shallow underground layers.

In order to identify the soil profile of PDCPT1, an image of an extensional crack with depth of around 2.5 m in a nearby cliff is shown in Fig. 14b. The soil stratification is clearly visible and less disturbed due to the downhill flow-slide. The surface layer is composed of 10–20 cm of organic soil followed by 30–40 cm of clay and silty clay

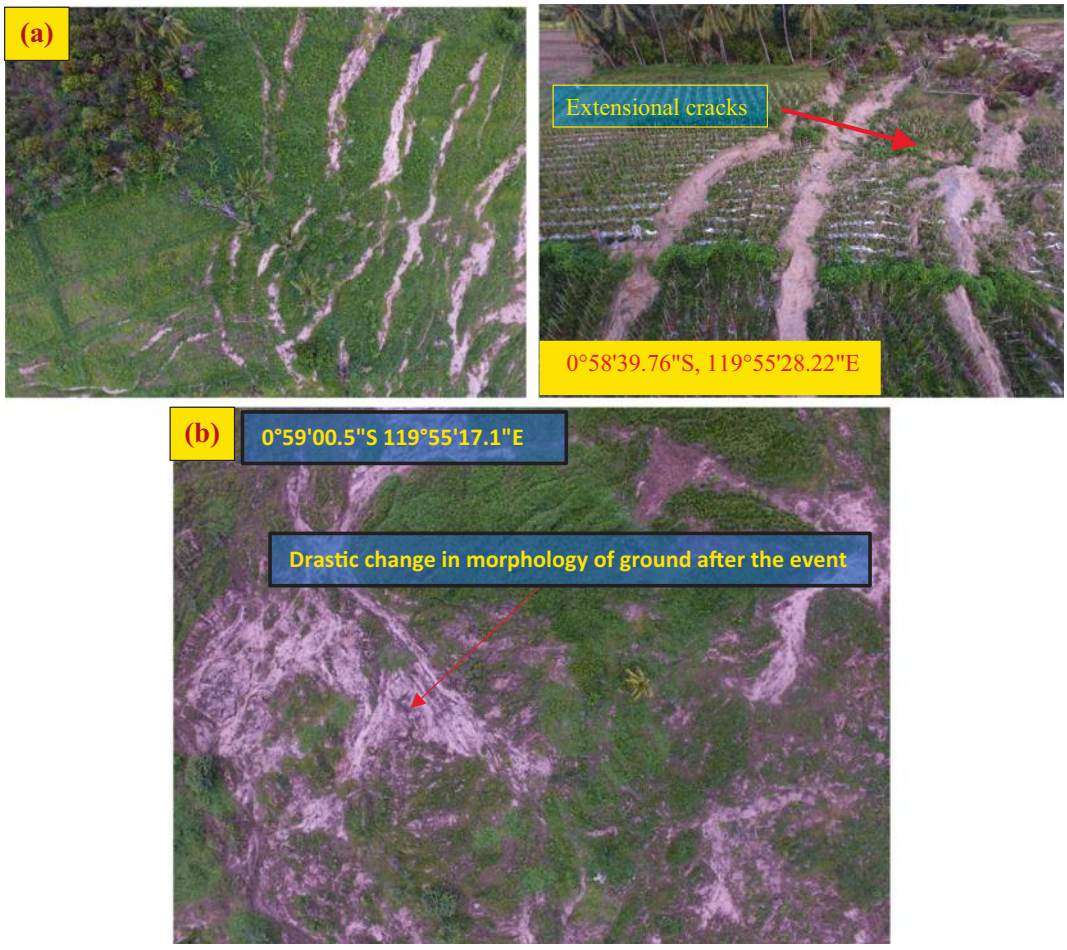

Fig. 12. Aerial imagery of damage within the failure Zones (a) extensional cracks in Zone (I) (b) flowslide and erosion of ground due to the mudflow Zone (II) (c) displacement of blue house in zone (II) (d) long distance transition of residential buildings after flowslide and mudflow (e) intersection of mudflow and stream.

Fig. 13. Locations of the PDCPT and collected soil samples at Jono-Oge.

layer. The underlying silty sand layer, which is between 10 and 20 cm in thickness, is sandwiched between the upper clayey layer and the lower clay silt layer, which is between 10 and 20 cm in thickness. Below the silty layer, there were several layers of sandy and gravelly sand layers which appeared to be affected by liquefaction in the underlying layers. As described in Kokusho (1999), it is possible that the presence of these low permeable layers at the top allowed the formation of a water film between them and the underlying gravelly sand layers. Some soil samples were collected from the exposed parts of extensional cracks, and the basic physical properties of soils in the stratified layers were determined.

3.2.2.2. Results from the tests conducted within the flow-slide zone. As shown in Fig. 13, the PDCPT 4, 5, 6, 8 were conducted alongside the damaged road that connects the North and South of flow-slide region. The locations and results of PDCPT 4, 5, 6 and 8 are shown in Fig. 15a~d. PDCPT4 was conducted beside the collapsed bridge in the North of Jono-Oge (Fig. 15a). PDCPT5 was conducted within the flow-slide Zone (I) (the tension zone), where there were many soil blocks which had been dragged along and had rafted together in failure area (Zone (II)) (the compression zone) (Fig. 15b). PDCPT6 was conducted in zone (II), where the flow-slide apparently started (Fig. 15c).

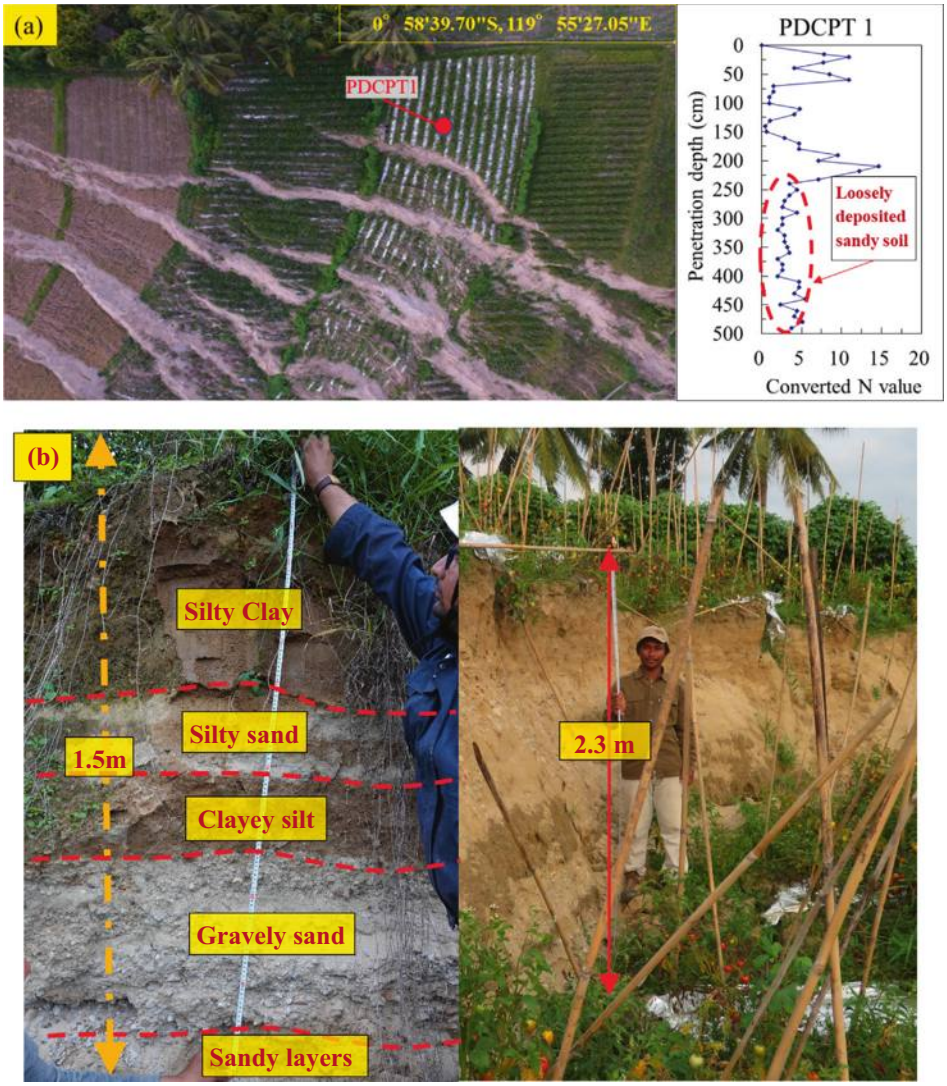

Fig. 14. PDCPT conducted within Zone (I) (a) Location and (b) test result at PDCPT1 (c) Profile of exposed soil layers at cliff created by extensional cracks.

PDCPT8 was conducted a few meters from the red building (Fig. 15d) which defied the ground movement and remained in its original position. Even though the building sustained considerable damage, rendering it uninhabitable, it did not experience displacement like the other structures in the flow-slide zone. This structure may have been able to resist the flow slide because of the massive raft foundation elaborated in Kiyota et al. (2020).

The N values obtained from all the PDCPTs for depths less than 5 m ranged between 5 and 10. These values indicate that the soils could be categorized as loose to very loose (USACE, 1994). These N values correspond to the critical Ncr values for soils categorized as potentially liquefiable at this range of depths (Koizumi, 1966). The soils appear to be loosely deposited sand and silty sand layers which were transported from the upstream of the flow-slide region. However, the resultant N-values from PDCPT 8 are greater than 10 beyond the depth of 3.5 m. That is, the N-values for PDCPT 8, which was conducted close the red house, were higher than for the other tests. A trend similar to PDCPT 8 was observed in the tests conducted by Kiyota et al. (2020) in the same vicinity. The out of trend peak in the results for in PDCPT 5 was attributed to the presence of a gravelly layer at 2.5 m, which appears to have been liquefied. According to historical records, the liquefaction of gravelly soils is rare. However, some cases of liquefaction in gravelly soils were observed in past earthquakes, such as during the 1995 Hyogoken Nambu earthquake, Japan, as well as during the 1983 Borah Peak earthquake in the United States, where extensive liquefaction took place in fluvial sandy gravel layers (Kokusho et al., 2004). It should be noted, however, that the lateral displacement and flow-slide in these earthquakes was between only a few meters and tens of meters. In the 2018 Sulawesi earthquake, the displacement of soil blocks was between a few meters to hundreds of meters. This

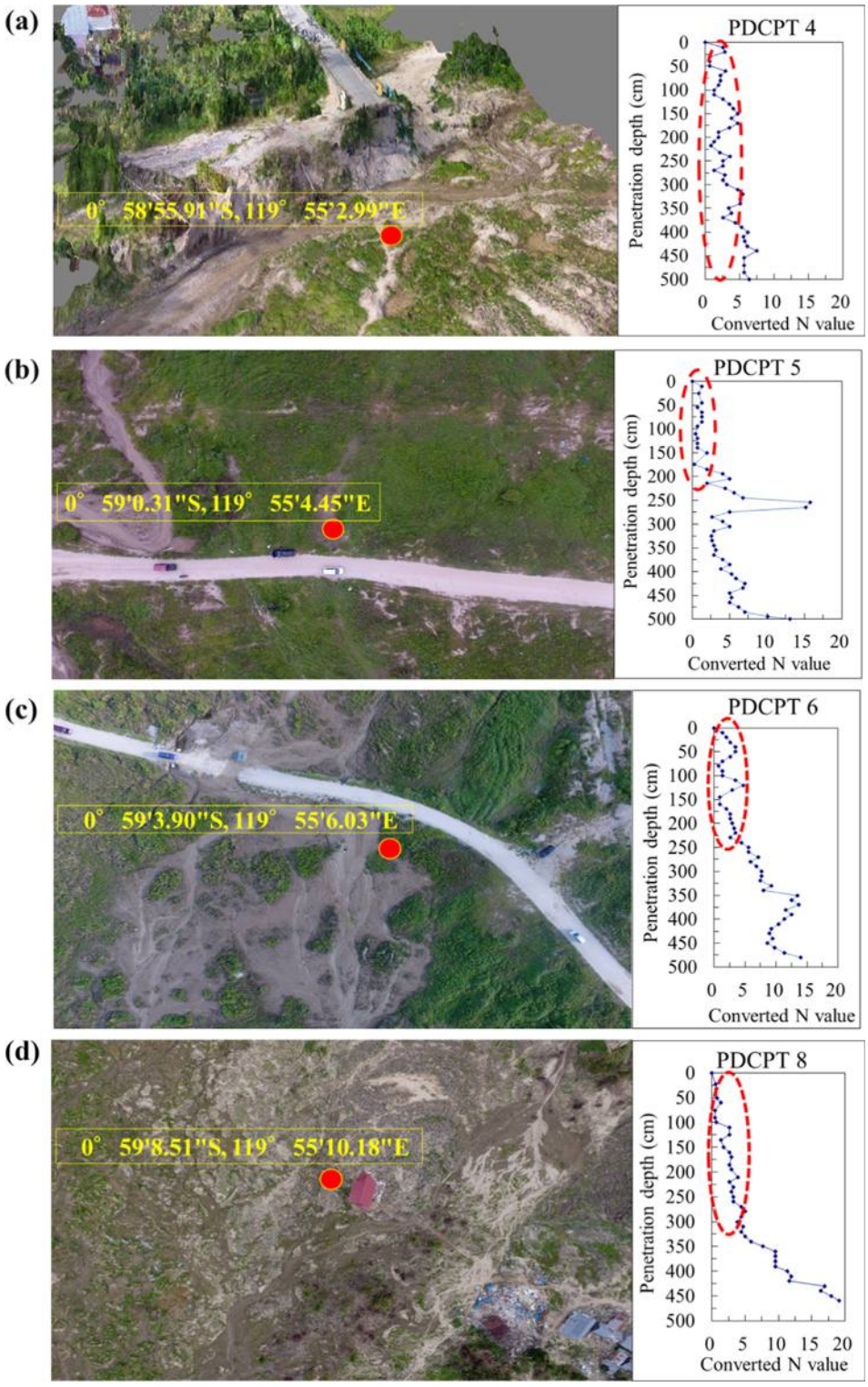

Fig. 15. Aerial imagery of locations of PDCPT and N_{SPT} versus depth values (a) PDCPT4 (b) PDCPT5 (c) PDCPT6 (d) PDCPT8.

was remarkable considering the very gentle slope of the ground and and that this area had no recorded history of liquefaction induced flow-slides.

3.2.3. Gradation of soil samples

Soil samples were collected from locations near the PDCPT tests in the failure zone as shown in Fig. 13 and were tested to determine the grain size distribution. The grain size distribution of soil samples S1, S3 and S5 are shown in Fig. 16. The soil in sample S1 can be classified as a uniform sand with traces of silt, while the soils in samples S3 and S5 can be classified as non-plastic silt (Japanese Geotechnical Society Standard, 2016). As seen in Fig. 16, soil sample S1 is the most liquefiable among the samples,

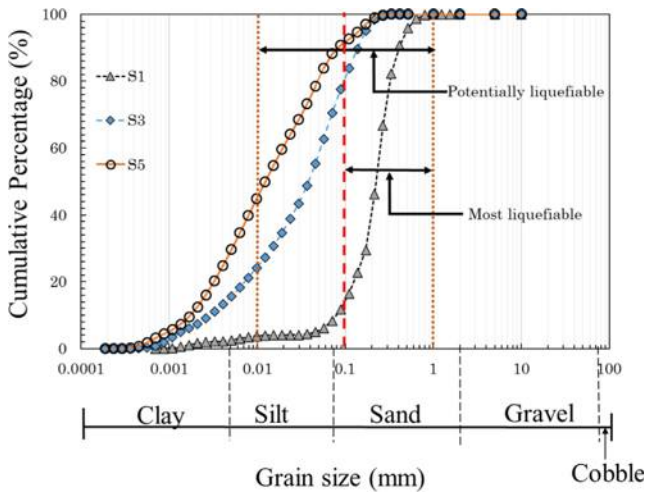

Fig. 16. Gradation of soil samples S1, S3 and S5 collected from the site.

whereasthe soils in samples S3 and S5 are potentially liquefiable soils, according to the soil classifications proposed by Tsuchida (1970). These soils were either transported by the flow slide, by the succeeding mudflow or deposited as residual soils. According to the handbook of Port and Harbor Research Institute of Japan (PHRI, 1997), the gradation of these soil samples indicates they are potentially liquefiable.

3.3. Probable mechanism of failure

According to interviews with eyewitnesses and video recordings of the flow-slides in the aftermath of the earthquake, flow failure started a minute after the earthquake had stopped first at the eastern side of Zone II. The flow-slide transported the soil blocks, houses and trees down the slope towards the Palu river at a relatively slow rate and deposited the residuals in Zone III. After the initial movement of ground in Zone II, the structure of the surrounding ground also failed, and it began flowing into the primary zone. The materials were carried distances of between a few tens of meters (Zone (I)) to around 1.5 km (Zone (II)) due to the flow-slide. Also, the breach of the irrigation channel resulted in mudflow into the area already affected by flow-slide. Interestingly, during the field investigations, the authors found that the surficial soil, which had been transported long distances by the flow-slide, behaved like a jelly after overnight rainfall and could not bear the static vertical load of an average human being. This is evidence of the very low static resistance of the displaced soil, and that the soil dilated under axial stress in saturated or partially saturated conditions.

The mechanism of the long-distance flow failure at Jono Oge is not yet clearly understood at this stage. There have been many theories and assumptions proposed by various researchers. Besides the complicated nature of the various factors involved in triggering the flow-slide, the resultant mudflow changed the morphology of the area through erosion, and removed the traces of flow-slides, making it difficult to propose a concrete hypothesis regarding the possible mechanism of failure. Kiyota et al. (2020) have proposed a hypothesis based on the assumption that the artisan pressure from the underlying confined aquifer triggered the flow-slide by reducing the effective stress along with the shear strength of the overlying ground surface. While the authors could not validate the presence of any such aquifer in their research, the JICA (2019) report substantiated the existence of a confined aquifer at a depth of about 30 m trough borehole tests, which is assumed to exist at a shallow depth. Also, it was observed from trenches excavated in the flow-slide zone that the sub-soil lithology was highly stratified with alternating layers of sand, sandy clay, silt, gravel, and organic soils, which reduced the effective permeability of the surface layers. The low permeability of the surface layers is thought to have inhibited the dissipation of excess water pressure despite the upwards pressure, which exceeded the critical hydraulic gradient from the confined aquifer.

Similar case of flow failure have been reported in the past in Lower San Fernando dam during the 1971 San Fernando earthquake, where failure occurred approximately 1 min after the ground ceased shaking (Seed, 1987). Kokusho (2003) summarized earthquake-triggered time-delayed flow failure cases, including the submarine landslide at Valdez as a result of the 1964 Alaskan earthquake. While the inertia force due to the earthquake is considered the biggest factor in such failures, there are many other contributing factors. For example, in the 1964 Niigata earthquake, the ground lithology based on bore-logs was found to be stratified with silty sub-layers sandwiched between loose sandy layers (Kishida, 1966). Furthermore, Kokusho and Fujita (2002) investigated the large lateral displacement of about 4 m following the 1964 Niigata earthquake in liquefied areas, despite the very gentle slope of the ground surface (less than 1%) and concluded that it was initiated by water-films of ultra-low shear resistance which appeared beneath low permeable silt seams sandwiched in clean sand deposits. In the case of Jono Oge, the presence of low permeable cap layers and underlying highly liquefiable sand and silty sand layers could be a factor in the failure of the ground. It may therefore be reasonable to suggest that an analogy can be drawn between this time earthquake and the 1964 Niigata earthquake. It is acknowledged that there has been no report of such a long-distance flow failure in the literature as that seen at Jono Oge.

A series of model tests conducted by previous researchers (Kokusho, 1999, 2016; Kokusho and Kojima, 2002), have revealed that liquefaction at a site with sandwiched lithology results in the liquified soil being trapped below the low permeability cap layer. This creates a thin interlayer of water, referred to as a "water film". The resulting inhibition of excess pore water pressure dissipation and presence of the water-film reduces the residual shear strength of the sandy soil layer to below the initial static

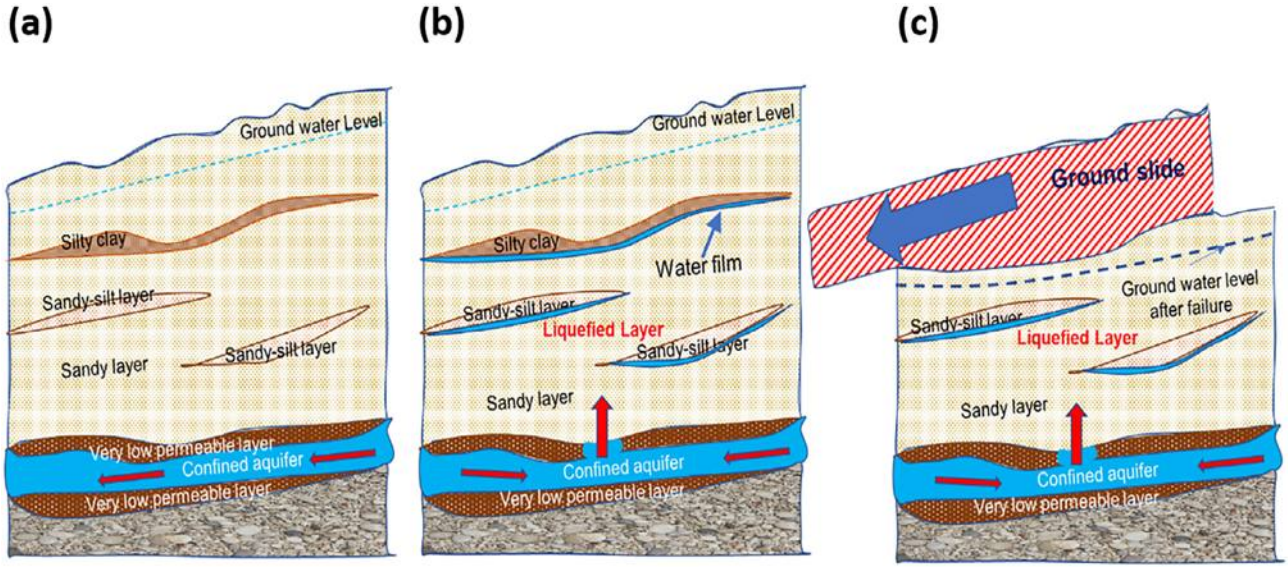

Fig. 17. The mechanism of flow slide and development of water film under low permeable layers (a) before the earthquake (b) immediately after initiation of liquefaction (c) after the earthquake.

shear stress. Consequently, even on a very gentle slope, lateral flow takes place due to the action of gravitational force until equilibrium is achieved. Note that the results of common laboratory tests have shown that such capping layers may not be continuous and that they do not necessarily spread horizontally across the whole failure zone.

The authors believe that complex factors were involved in the triggering of the large-scale flow-slide at Jono-Oge on a very gentle sloping ground, which continued even after the seismic ground motion ceased. The combined effects of typical geology and the terrain, the formation of a water film due to liquefaction of the sandy layer overlain by capping layer, and the existence of underlying artesian aquifer may all have played a role in the long-distance flow-slide at Jono-Oge (Fig. 17a~c). The presence of a confined aquifer at a shallow depth and water springs in the Balaroa and Petobo flow-slide zone, which was confirmed by Kiyota et al. (2020), may also have contributed to the flow-slide.

4. Conclusions and recommendations

This paper presents a preliminary report on the geotechnical damage brought by the 2018 Sulawesi earthquake based on the results of a reconnaissance survey and subsequent data analyses and their interpretations. Much of the damage to infrastructures was caused by liquefaction induced long distance flow-slides in Balaroa, Petobo, Jono-Oge and Sibalaya areas of Palu city.

The focus of this report was on the Jono-Oge area, where the flow-slide was the longest. The authors collected information using a number of different surveying methods, including the use of a GPS device, cameras, and UAV. Furthermore, the ground condition in the affected areas was investigated by in-situ testing, including PDCP tests and soil sampling (both disturbed and undisturbed).

The image data collected by UAV and satellite images were used to evaluate the large-scale displacements at flow-slide area and explain the mechanism of failure. Based on the information gathered in this research, the following conclusions could be drawn:

- The geological morphology of central Sulawesi as well as magnitude and scale of extreme event caused by an earthquake at the Palu-Koro fault were found contributed to the severity of the geotechnical failures, such as liquefaction the induced flow-slides and the distance of the flow-slides.
- Considering the geological features of Sulawesi region, it can be concluded that all major flow-slides in the Palu valley occurred at locations where a new alluvial fan meets an old alluvial fan.
- The presence of low permeable layers (silt and clay) over loosely deposited sandy and sandy gravel layers suggests the complex mechanism of the long-distance flow-slide at Jono-Oge can be explained by the interlayer water film theory. Furthermore, it is assumed that damage to the underlying artesian aquifer during the earthquake may also have contributed to the development of the water film and the liquefaction induced flow-slide in the layers with very low mobilized shear resistance (nearly zero).
- Further research, including geophysical tests as well as laboratory tests and physical modeling, is required to determine the actual mechanism of such flow failures, and to suggest preventive measures against future geohazard risks in areas with similar geological features.

Acknowledgement

The authors would like to express their sincere gratitude to the members of the JICA domestic committee for technical support to the 2018 Sulawesi Earthquake, Indonesia. Particular thanks is extended to Prof. Kenji Ishihara, Prof. Takaji Kokusho, Prof. Susumu Yasuda, Prof. Ikuo Towhata, Prof. Mitsu Okamura, Dr. Takashi Kiyota and Dr. Kimio Takeya for their valuable comments and suggestions. The authors also would like to acknowledge JICA for the partial support provided in the initial phase of the investigation. Special thanks go also to Dr. Naoto Tada, JICA Indonesia, for his encouragement and timely support during the investigation. Last but not least, we are grateful to Ms. Ode Wa Sumartini, a graduate student at Kyushu University and the students of Tadulako University, Palu, for their help and support during the field investigations.

References

Andrus II, R.D., Stokoe II, K.H., 2000. Liquefaction resistance of soils from shear-wave velocity. J. Geotech. Geoenviron. Eng. 126 (11), 1015–1025.

Bardet, J.-P., Tobita, T., Mace, N., Hu, J., 2002. Regional modeling of liquefaction-induced ground deformation. Earthquake Spectra 18 (1), 19–46.

Boulanger, R.W., Wilson, D.W., Idriss, I.M., 2012. Examination and reevalaution of spt-based liquefaction triggering case histories. J. Geotech. Geoenviron. Eng. 138 (8), 898–909.

Bradley, K., Mallick, R., Andikagumi, H., Hubbard, J., Meilianda, E., Switzer, A., Du, N., Brocard, G., Alfian, D., Benazir, B., Feng, G., Yun, S., Majewski, J., Wei, S., Hill, E.M., 2019. Earthquake-triggered 2018 Palu valley landslides enabled by wet rice cultivation. Nat. Geosci. 12, 935–939.

Cetin, K.O., Bilge, H.T., Wu, J., Kammerer, A.M., Seed, R.B., 2009. Probabilistic model for the assessment of cyclically induced reconsolidation (volumetric) settlements. J. Geotech. Geoenviron. Eng. 135 (3), 387–398.

Cetin, K.O., Seed, R.B., Kiureghian, A.D., Tokimatsu, K., Harder, L.F., Kayen, R.E., Moss, R.E.S., 2004. Standard penetration test-based probabilistic and deterministic assessment of seismic soil liquefaction potential. J. Geotech. Geoenviron. Eng. 130 (12), 1314–1340.

Cubrinovski, M., Robinson, K., Taylor, M., Hughes, M., Orense, R., 2012. Lateral spreading and its impacts in urban areas in the 2010–2011 Christchurch earthquakes. N. Z. J. Geol. Geophys. 55 (3), 255–269.

Cummins, P.R., 2019. Irrigation and the Palu landslides. Nat. Geosci. 12, 881–882.

El May, M., Kacem, J., Dlala, M., 2009. Liquefaction susceptibility mapping using geotechnical laboratory tests. Int. J. Environ. Sci. Technol. 6 (2), 299–308.

Goda, K., Mori, N., Yasuda, T., Prasetyo, A., Muhammad, A., Tsujio, D., 2019. Cascading geological hazards and risks of the 2018 Sulawesi Indonesia earthquake and sensitivity analysis of tsunami inundation simulations. Front. Earth Sci. 7 (261).

Hall, R., 2014. Indonesian tectonics: subduction, extension, provenance and more. Indonesian Petroleum Association, Proceedings of the 38th Annual Convention, IPA14-G-360, August, 1–43.

Heidarzadeh, M., Muhari, A., Wijanarto, A.B., 2019. Insights on the source of the 28 september 2018 Sulawesi tsunami, Indonesia based on spectral analyses and numerical simulations. Pure Appl. Geophys. 176 (1), 25–43. https://doi.org/10.1007/s00024-018-2065-9.

Japanese Geotechnical Society Standard, 2016. Method for portable dynamic conepenetration test (JGS 1433-2012).

JICA, 2019. Report of the technical committee on The 2018 Sulawesi earthquake, Indonesia, Japan International Corporation Agency (JICA).

Japanese Geotechnical Society Standard, 2016. Method of classification of geomaterials for engineering purposes (JGS 0051-2009).

Juang, C.H., Ching, J., Wang, L., Khoshnevisan, S., Ku, C.-S., 2013. Simplified procedure for estimation of liquefaction-induced settlement and site-specific probabilistic settlement exceedance curve using cone penetration test (CPT). Can. Geotech. J. 50 (10), 1055–1066.

Kishida, H., 1966. Damage to reinforced concrete buildings in Niigata City with special reference to foundation engineering. Soils and Foundations 6 (1), 71–88.

Kiyota, T., Furuichi, H., Hidayat, R.F., Tada, N., Nawir, H., 2020. Overview of long-distance flow-slide caused by the 2018 Sulawesi earthquake, Indonesia. Soils Foundat. https://doi.org/10.1016/j.sandf.2020.03.015.

Koizumi, Y., 1966. Changes in density of sand subsoil caused by the Niigata earthquake. Soils Found. 6 (2), 38–44.

Kokusho, T., 1999. Water film in liquefied sand and its effect on lateral spread. J. Geotech. Geoenviron. Eng. 125 (10), 817–826. https://doi.org/10.1061/(ASCE)1090-0241(1999)125:10(817).

Kokusho, T., Fujita, K., 2002. Site investigation for involvement of water films in lateral flow in liquefied ground. J. Geotech. Geoenviron. Eng. 128 (11), 917–925.

Kokusho, T., 2003. Current state of research on flow failure considering void redistribution in liquefied deposits. Soil Dyn. Earthq. Eng. 23, 585–603.

Kokusho, T., 2016. Major advances in liquefaction research by laboratory tests compared with in situ behavior. Soil Dyn. Earthq. Eng. 91, 3–22. https://doi.org/10.1016/j.soildyn.2016.07.024.

Kokusho, T., Hara, T., Hiraoka, R., 2004. Undrained shear strength of granular soils with different particle gradations. J. Geotech. Geoenviron. Eng. 130 (6), 621–629. https://doi.org/10.1061/(ASCE)1090-0241(2004)130:6(621).

Kokusho, T., Kojima, T., 2002. Mechanism for postliquefaction water film generation in layered sand. J. Geotech. Geoenviron. Eng. 128 (2), 129–137. https://doi.org/10.1061/(ASCE)1090-0241(2002)128:2(129).

Mason, B., Gallant, A., Hutabarat, D., Montgomery, J., Reed, A., Wartman, J., Irsyam, M., Prakoso, W., Djarwadi, D., Harnanto, D., Alatas, I., Rahardjo, P., Simatupang, P., Kawanda, A., Hanifa, R., 2019. Geotechnical reconnaissance: The 28 September 2018 M7.5 Palu-Donggala, Indonesia earthquake,GEER Association Report No. GEER-061. https://doi.org/10.18118/G63376

Mikami, T., Shibayama, T., Esteban, M., Takabatake, T., Nakamura, R., Nishida, Y., Achiari H., Rusli., Marzuki, A.G., Marzuki, M.F.H., Stolle, J., Krautwald, C., Robertson, I., Aránguiz, R., Ohira, K., 2019. Field survey of the 2018 Sulawesi tsunami: inundation and run-up heights and damage to coastal communities. Pure Appl. Geophys. (June). https://doi.org/10.1007/s00024-019-02258-5.

Moss, R.E., Seed, R.B., Kayen, R.E., Stewart, J.P., Kiureghian, A.D., Cetin, K.O., 2006. CPT-based probabilistic and deterministic assessment of in situ seismic soil liquefaction potential. J. Geotech. Geoenviron. Eng. 132 (8), 1032–1051.

Maulana, Adi., Imai, Akira., Watanabe, Koichiro., Yonezu, Kotaro., Nakano, Takanori., Boyce, Adrian., Page, Laurence., Anders, Scher-sten., 2016. Origin and geodynamic setting of Late Cenozoic granitoids in Sulawesi, Indonesia. J. Asian Earth Sci. 124, 102–125. https://doi.org/10.1016/j.jseaes.2016.04.018.

Moss, R.E.S., Kayen, R.E., Tong, L.Y., Liu, S.Y., Cai, G.J., Wu, J., 2011. Retesting of liquefaction and nonliquefaction case histories from the 1976 Tangshan earthquake. J. Geotech. Geoenviron. Eng. 137 (4), 334–343.

Ohsumi, T., Hazarika, H., Hara, T., Kuribayashi, K., Kuroda, S., Takezawa, K., Furuichi, H., 2016. Analysis of coastal structure damaged by the 2011 off the Pacific coast of Tohoku earthquake - field

investigation and numerical simulation. Japanese Geotechn. Soc. Special Publ. 2 (73), 2498–2503.
Okamura, M., Ono, K., Minaka, U.S., Arsyad, A., Nurdin, S., 2020. Large scale flow side in Sibalaya - A consequence of the 2018 Sulawesi Earthquake, Indonesia. Soils and Foundations 60 (4), 1050–1063.
Omira, R., Dogan, G.G., Hidayat, R., Husrin, S., Prasetya, G., Annunziato, A., Proietti, C., Probst, P., Paparo, M.A., Wronna, M., Zaytsev, A., Pronon, P., Giniyatullin, A., Putra, P.S., Hartanto, D., Ginanjar, G., Kongko, W., Pelinovsky, E., Yalciner, A.C., 2019. The September 28th, 2018, tsunami In Palu-Sulawesi, Indonesia: a post-event field survey. Pure Appl. Geophys. 176 (4), 1379–1395. https://doi.org/10.1007/s00024-019-02145-z.
Port Harbour Research Institute of Japan, 1997. Handbook on Liquefaction Remediation of Reclaimed Land. A.A Balkema, Rotterdam.
Seed, H.B., 1987. Design problems in soil liquefaction. J. Geotech. Eng. ASCE 113 (8827–8845).
Socquet, A., Simons, W., Vigny, C., McCaffrey, R., Subarya, C., Sarsito, D., Ambrosius, B., Spakman, W., 2006. Microblock rotations and fault coupling in SE Asia triple junction (Sulawesi, Indonesia) from GPS and earthquake slip vector data. J. Geophys. Res. Solid Earth 111 (8), 1–15. https://doi.org/10.1029/2005JB003963.
Socquet, A., Hollingsworth, J., Pathier, E., Bouchon, M., 2019. Evidence of supershear during the 2018 magnitude 7.5 Palu earthquake from space geodesy. Nat. Geosci. 12 (3), 192–199.
Thein, P.S., Pramumijoyo, S., Brotopuspito, K.S., Kiyono, J., Wilopo, W., Furukawa, A., Setianto, A., Putra, R.R., 2015. Estimation of s-wave velocity structure for sedimentary layered media using micro-tremor array measurements in Palu city, Indonesia. Procedia Environ. Sci. 28 (SustaiN 2014), 595–605. https://doi.org/10.1016/j.proenv.2015.07.070.
Tsuchida, H., 1970. Prediction and countermeasure against liquefaction in sand deposits. In: The Seminar of the Port and Harbour Research Institute, Yokosuka: Ministry of Transport, Japan, January, pp. 3.1–3.33
U.S. Army Corps of Engineering, 1994. Design of sheet pile walls, Engineer Manual, EM 1110-2-2504, U.S. Army Corps of Engineers, Department of the Army. Washington D.C., USA.
U.S. Geological Survey, 2018. M 7.5 - 70km N of Palu, Indonesia. Retrieved March 22, 2019, from https://earthquake.usgs.gov/earthquakes/eventpage/us1000h3p4/map.
Valverde-Palacios, I., Vidal, F., Valverde-Espinosa, I., Martín-Morales, M., 2014. Simplified empirical method for predicting earthquake-induced settlements and its application to a large area in Spain. Eng. Geol., 18158–18170
van Leeuwen, T., Allen, C.M., Elburg, M., Massonne, H.J., Palin, J.M., Hennig, J., 2016. The Palu metamorphic complex, NW Sulawesi, Indonesia: origin and evolution of a young metamorphic terrane with links to Gondwana and Sundaland. J. Asian Earth Sci. 115, 133–152. https://doi.org/10.1016/j.jseaes.2015.09.025.
Watkinson, I.M., Hall, R., Cottam, M.A., Wilson, M.E.J., 2011. Ductile flow in the metamorphic rocks of central Sulawesi. The SE Asian Gateway: History and Tectonics of the Australia-Asia Collision. Geological Society of London.
Watkinson, I.M., Hall, R., 2019. Impact of communal irrigation on the 2018 Palu earthquake-triggered landslides. Nature Geoscences. 12, 940–947.
Youd, T.L., Hansen, C.M., Bartlett, S.F., 2002. Revised multilinear regression equations for prediction of lateral spread displacement. J. Geotech. Geoenviron. Eng. 128 (12), 1007–1017.